

# A Flying Anemometer Quadrotor: Part 1

S. Prudden,\* A. Fisher, A. Mohamed, and S. Watkins.  
RMIT University, Melbourne, Australia

## ABSTRACT

The feasibility of using a Multi-rotor Unmanned Aerial System (MUAS) as flying anemometers for measurement of wind in urban environments was investigated. Flow mapping was conducted around the MUAS using smoke flow visualisation and multi-hole pressure probes to analyse the effects of the propellers on the measured flow speed and direction and determine a suitable mounting location for an on-board multi-hole pressure probe sensor system. It was determined that propeller-induced effects extended beyond a feasible on-board probe length. Therefore correction factors were developed from experimental measurements for application to the output of the on-board multi-hole pressure probe.

## NOMENCLATURE

X	Longitudinal measurement position (mm)
$\alpha$	Propeller-induced flow deflection angle (degrees)
$\Phi$	MUAS angle of attack (degrees)
u	Flow speed (m/s)
V	Flow velocity (m/s)
$\omega$	Angular velocity (rad/s)
$\lambda$	Tip speed ratio
r	Propeller radius (m)

## 1 INTRODUCTION

Knowledge of wind flow around buildings has a number of useful applications in architecture and construction industries. Wind data can be used to optimise the locations of wind turbines and photovoltaic cells on buildings in urban and city environments, assess effects of flow separation on structural integrity as well as investigate the feasibility of Micro Aerial Vehicles (MAVs) soaring at the tops of tall buildings [1, 2, 3, 4].

Measuring wind flow around buildings presents a number of practical challenges due to the size and complexity of the structures and frequently wind tunnel small scale models and wind tunnel are used, however this method can be expensive and time consuming [5]. When analysing complex turbulent flows, assumptions and simplifications must be made. Computational Fluid Dynamics (CFD) has an advantage in that a

large number of combinations of tests can be conducted at a small portion of the cost of using a wind tunnel. However, they require extensive computing power and the resolutions are limited [6].

In-situ measurements of flow around buildings have been traditionally undertaken using static sensors fixed to masts and/or the structure being analysed. Atmospheric measurements for flow mapping require sample times of the order of minutes at discrete point locations in order to resolve for low frequency wind oscillations. Some forms of atmospheric boundary layer measurements also require multiple simultaneous measurements [3]. This introduces practical limitations, as multiple probes require significant time and resources to mount. LIDAR can be used to provide ground-based remote wind measurement of altitudes up to 200m [7]. However these are expensive, suffer from limited resolution and produce spatially-averaged results over a relatively large sensing area [8]. There is an opportunity to utilise Multi-rotor Unmanned Aerial System (MUAS) as "flying anemometers".

MUAS have the advantage over fixed-wing UAS due to their ability to move in all directions, hover at a fixed location in space and take off and land vertically. This makes them more suitable for taking point measurements close to buildings and flying in confined urban environments. MUAS have demonstrated the ability to carry sensors for precision 3D mapping in confined spaces of both forests and mineshafts [9, 10].

Existing research projects have investigated measuring the MUAS dynamic behaviour or differential power measurements to estimate wind fields to a limited resolution [11, 12, 13]. The miniaturisation of flow sensors, such as pressure or ultrasonic-based sensors, have allowed these payloads to have a minimal impact on the MUAS airframe size, weight and performance. Distributed pressure sensors and sonic anemometers have been investigated as onboard sensors for path planning and atmospheric measurements respectively [14, 15]. However the effects of propeller wake on on-board wind measurements are not well understood. A major focus of existing propeller wake studies in hover and forward flight has been on the regions underneath or downstream of the rotors, which are obviously unsuitable for flow sensors. Mounting positions above, or in front, of the MUAS airframe might remain upstream of the major rotor wash when using a suitable control system. Therefore the potential rotor-induced effects in these regions must be well-understood and characterised in order to accurately measure atmospheric flows.

In this paper we explore the feasibility of using an MUAS as a wind-sensing platform to accurately resolve atmospheric

\*Email address: sam.prudden@gmail.com

flow vectors at point locations. MUAS have potential advantages over ground- and pole-mounted sensors because they can be quickly relocated to measure wind at multiple locations. Advances in autonomous control systems may also allow for swarms of MUAS to sense multiple locations in real time for flow mapping, such as measuring vertical velocity or intensity profiles. Additional applications for on-board flow sensing on MUAS may extend to measuring the upstream flow to assist reducing perturbations in gust, such as the phase-advanced attitude control system demonstrated for fixed-wing MAVs by Mohamed [16].

In this paper there is a preliminary analysis of the induced effects of MUAS propellers on the incident flow field in front of the airframe using Multi Hole Pressure Probes (MHPP). Qualitative flow visualisation and quantitative flow mapping were used to determine the induced flow angle and speed in a range of flight profiles. These measurements could then be used to identify a suitable mounting location for an on-board forward facing multi-hole pressure probe (MHPP) as well as identify limitations and required corrections. The research in this paper forms part of a series of studies that include development and integration of a purpose-built lightweight MHPP system as well as airborne wind measurement testing.

## 2 EXPERIMENTAL SETUP

### 2.1 Test Platform

The MUAS platform used in this project has been designed to accommodate both wind tunnel and flight testing. The platform is a quad-rotor configuration with diagonal rotor spacing of 800mm and a take-off weight of 2.4kg. The propellers have a diameter of 330mm and pitch of 119mm. The airframe has been designed to mount a forward-facing mount for a Multi-Hole Pressure Probe (MHPP) in line with the longitudinal axis of the Inertial Measurement Unit (IMU) to enable the measurements to be taken upstream of the rotor wash and reduce the complexity of attitude corrections when resolving the MHPP in the body-fixed coordinate frame (BCF) to the global coordinate frame (GCF). Methods used to resolve the flow vectors to the GCF during flight will be covered in Part B of this research. The MHPP has been developed at RMIT and has a 90 degree cone of acceptance to allow the large turbulence fluctuations in urban environments to be captured, as found by Milbank et al [17]. It is assumed that in the flying configuration the closed loop control system will adjust the heading angle to ensure that the mean wind vectors remain within the sensor cone of acceptance. The MHPP longitudinal mounting position can be adjusted to make use of the flow mapping results and place the probe in the position where it is least severely affected by propeller wash but not impeded by structural stiffness or vibration, as demonstrated by de Boisblanc [15].

The implications and method of resolving wind measurements from a moving platform will be covered in a future paper.

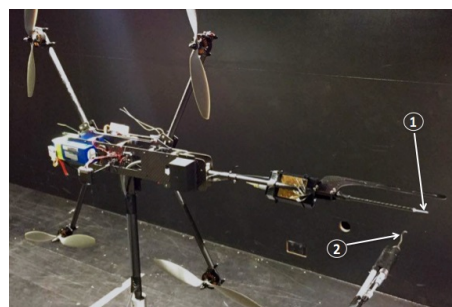


Figure 1: The mounted MUAS showing the on-board MHPP mounting configuration (1), and the Cobra Probe MHPP used for flow mapping (2)

### 2.2 Wind Tunnel Setup

The RMIT Industrial Wind Tunnel uses a return cycle configuration and has a test section of 9 x 3 x 2m. The base turbulence intensity of the tunnel is 1.5% [18]. The MUAS was held on its right side on a static sting. This orientation allowed the MUAS to be held out of ground effect while minimizing the length of the sting, thus optimizing the stiffness of the rig. The sting could also be rotated axially to investigate the effects of pitch and roll on flow measurements, thus replicating hover conditions in a constant wind speed or forward flight.

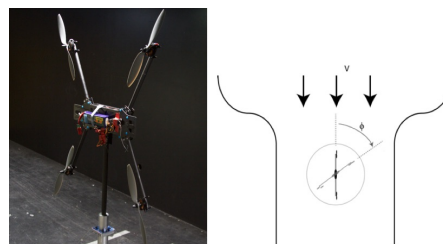


Figure 2: Wind tunnel mounting configuration

A TFI Cobra Probe [19] was used to measure local flow speed, angle and turbulence intensity at a range of longitudinal positions.

## 3 RESULTS AND DISCUSSION

Extensive wind tunnel testing was conducted to map the flow field along the longitudinal axis in front of the MUAS airframe. This was done to investigate the minimum distance required to avoid propeller-induced effects. This information was utilised to identify the most suitable position for the MHPP in front of the airframe. Quantitative flow measurements were conducted using a Cobra Probe at 1000Hz for 28 seconds in order allow both high and low frequency fluctuations to be analysed. Measurements were taken at least three times per configuration for repeatability and flow angles measured in each configuration were found to have an error within  $\pm 1$  degree.

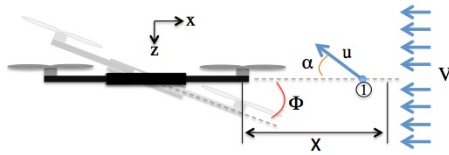


Figure 3: Parameters analysed in flow mapping experiments

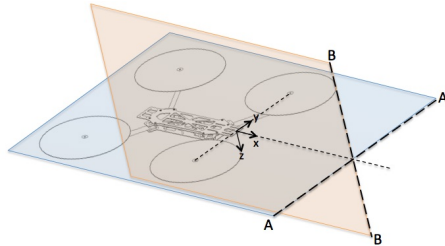


Figure 4: Flow visualisation planes

The parameters analysed in these experiments are shown in Figure 3.  $X$  represents the longitudinal distance for flow measurements forwards of the rotor hub axis.  $\Phi$  is the MUAS angle of attack in degrees and  $V$  is the tunnel velocity in metres per second. If we consider any point in the flow, such as point 1 on Figure 3,  $\alpha$  and  $u$  represent the propeller-induced deflection angle (degrees) and flow speed (metres per second) measured by the Cobra Probe. As shown in Figure 4, AA represents the smoke wire mounting orientation in the lateral plane, where the wire is level with the propeller axis. BB represents the smoke wire in the vertical plane, where the wire is at the mid-point between the rotor hubs. Both wires were placed at approximately  $X=2r$ . The MHPP was designed to be mounted in line with the longitudinal axis of the flight controller and level with the propeller hubs in the  $z$ -axis. Therefore, due to the scope of this project, quantitative flow measurements were not conducted at a range of positions in the  $z$ -axis and instead focused purely on the longitudinal axis. Analysis of flow fields at additional locations may be conducted in future research.

### 3.1 Effects of Reynolds Number

The deflection angle,  $\alpha$ , is a function of tip speed ratio,  $\lambda$ , and Reynolds number.  $\lambda$  is a dimensionless ratio between the angular velocity of the propellers and the linear velocity of the air, as shown in Equation 2. An initial experiment was conducted to assess the effect of the Reynolds numbers within the test matrix. This was conducted by varying the tunnel flow speed and propeller RPM to produce the same tip speed ratio and measuring the flow deflection. Measurements were taken at longitudinal positions of  $X=200, 300, 400$  and  $500$ mm. The ratios are shown in Table 1. The ratios were selected to operate between the limits of the Cobra Probes minimum velocity and the maximum thrust able to

be safely contained on the MUAS sting. The flow deflection was found by measuring the flow speed and angle with the propellers stationary and spinning in order to account for the initial mounting angle.

$$\alpha = f(\lambda, Re) \quad (1)$$

$$\lambda = \frac{\omega r}{V} \quad (2)$$

Wind Speed (m/s)	Propeller RPM	Tip Speed Ratio ( $\lambda$ )
4.17	2500	5.18
6	3600	5.18
7	4200	5.18

Table 1: Variables used to assess the effects of Reynolds number

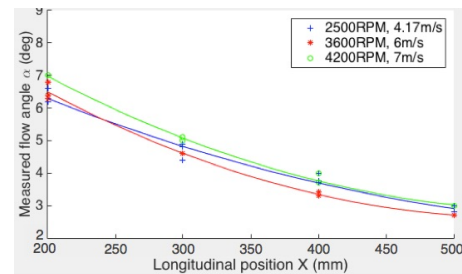


Figure 5: Flow measurements at three combinations of  $V$  and  $\omega$  for  $\lambda=5.18$

With a constant  $\lambda$ , the resultant deflection angle measured at each  $X$  position demonstrated less than 1 degree of variation between the three test configurations. This indicates that the Reynolds numbers did not significantly influence the deflections, thus allowing a uniform RPM to be used for all tests. In order to identify the propeller RPM at hover, the motor/propeller system used in the MUAS was first analysed using a force balance and the thrust curve was identified. The thrust of four propellers required to lift the weight of the MUAS platform corresponded to 3600RPM. This value was subsequently used for all further testing.

### 3.2 Propeller Flow Visualisation

Flow visualisation was used to qualitatively measure the induced effects of the propellers on the incident flow upstream of the airframe, which is a region that has seen very little analysis in previous research. The aim was to gain an understanding of the maximum distance significantly influenced by the propellers, the regions most severely affected as well as the amount of induced turbulence and flow mixing along the longitudinal axis where an on-board MHPP would be mounted. Two planes were analysed, as demonstrated in



Figure 4. In both tests the MUAS had zero pitch and yaw angle relative to the tunnel flow and equal thrust was generated from all four propellers. Smoke was generated using a heated wire covered in mineral oil. The tunnel flow speed was held at 5km/h to prevent excessive smoke dissipation. The turbulence intensity of the wind tunnel combined with vortex shedding from the smoke wire caused some visible turbulence in the baseline tests with stationary propellers. The propellers were spun at 830RPM in order to maintain a tip speed ratio of 5.18, which corresponded with all quantitative tests.

The streamlines in the lateral plane, shown in Figure 6, demonstrated significant lateral displacement, with the angle,  $\theta$ , increasing along both the longitudinal and lateral axes towards the airframe and propellers respectively. The streamlines approximately  $\pm 30\text{mm}$  from the centreline of the airframe demonstrated very little deflection, indicating that the wakes of the left and right propellers do not interact in this configuration. Despite being turned outwards, the streamlines also appeared to remain relatively laminar until reaching downstream of the vortices caused by the propellers and front arms.

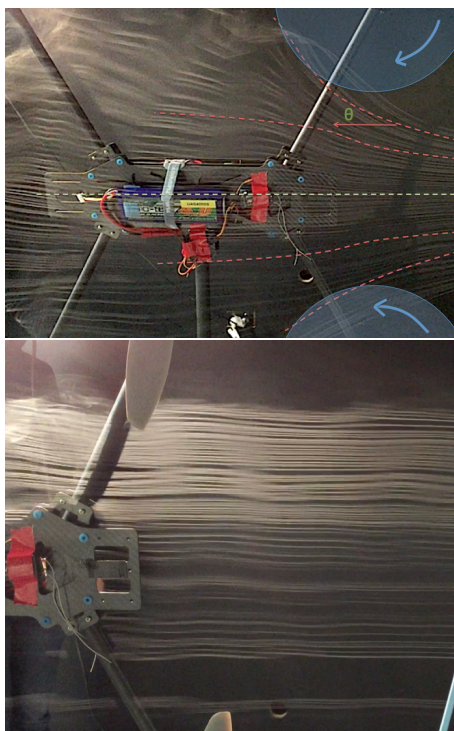


Figure 6: Smoke flow results in the lateral plane with propellers spinning (top) and stopped (bottom)

The streamlines in the vertical plane, shown in Figure 7, also demonstrated significant vertical displacement within a distance of 300mm from the rotor hub axis. The streamlines approximately 100mm above and below the propeller axis demonstrated similar deflection angles. It can also be

noted that because the smoke streamlines passed equidistant between the tandem rotors, the maximum amount of flow deflection was experienced at a position towards the rear of the rotor, unlike a single rotor that creates a stream-tube near the leading edge of the rotor. Relatively laminar flow was observed upstream of the rotor hub axis. The flow also appeared to develop a boundary layer over the airframe.

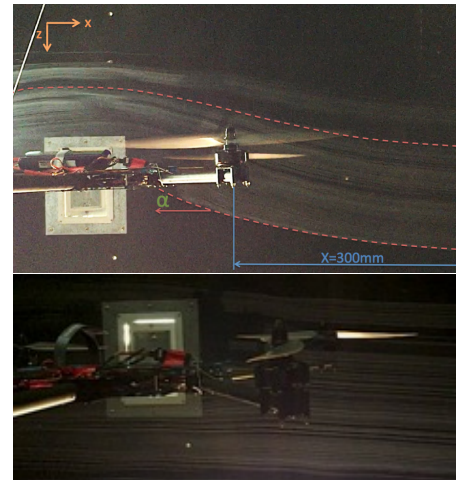


Figure 7: Smoke flow results in the vertical plane with propellers spinning (top) and stopped (bottom)

These images indicated that the region approximately two rotor radii upstream of the rotor hub axis is unsuitable for mounting a MHPP due to the significant propeller-induced flow angle. Therefore a MHPP cannot be mounted directly to the airframe on the longitudinal axis and will instead require an extended mount to place it further forwards. The smoke flow did not provide an indication of whether the propellers had increased the flow speed, however it did demonstrate that the propellers caused little increase in turbulence upstream of the rotor hub axis. This experiment also did not account for a range of incident wind angles in pitch and yaw.

### 3.3 Quantitative analysis of propeller-induced airflow deflection

#### 3.3.1 Propeller Influence Region

An experiment was conducted to identify the maximum longitudinal distance in front of the MUAS where the flow was influenced by the propellers to determine the minimum probe length required to avoid these effects. This test was first conducted at  $V=6\text{m/s}$  and an MUAS angle of attack of 0, 15 and 30 degrees. Measurements were taken between  $X=0\text{mm}$  and  $X=800\text{mm}$  in 100mm increments.

The propeller-induced flow deflection,  $\alpha$ , was found to increase exponentially as  $X$  was reduced and the probe was brought closer to the propellers. A position of  $X=0\text{mm}$  the deflection reached approximately 14 degrees. These quantitative measurements reflected the smoke flow images presented

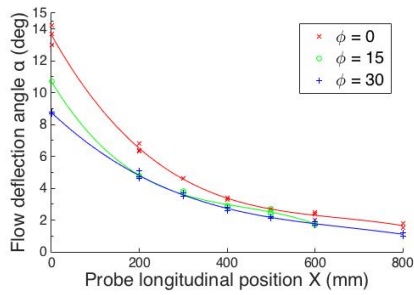


Figure 8: Flow deflection at  $\lambda=5.18$

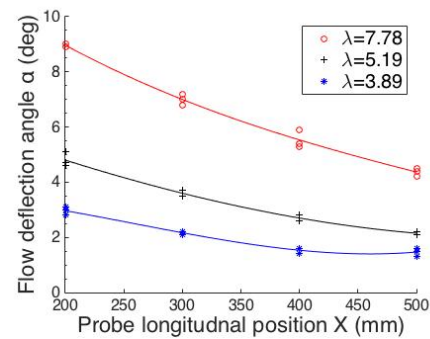


Figure 10: Flow deflection at  $\Phi=30$  deg

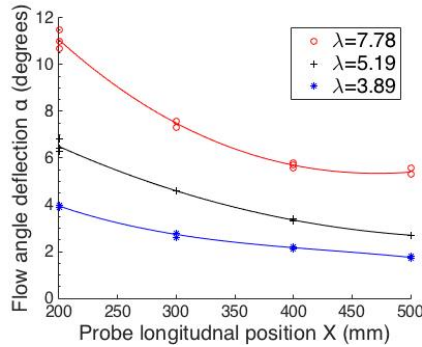


Figure 9: Flow deflection at  $\Phi=0$  deg

in Figure 3.2.

It was determined that the propellers influenced the flow beyond a distance of  $X=800\text{mm}$  albeit at a relatively small angle.  $X=800\text{mm}$  represents a probe length that is approximately 250% longer than the MUAS airframe and 6.7 radii forwards of the rotor hub axis. Mounting a probe this far in front of the MUAS would most likely introduce structural implications such as flex and a weight penalty caused by the probe mounting structure, difficulty achieving an ideal centre of gravity as well as impeding the manoeuvrability of the MUAS. Therefore measurements beyond this position were not tested. As a result, passively avoiding the propeller induced effects on flow measurements by placing the probe further forward was deemed impractical.

Additional measurements were taken at  $X=200, 300, 400$  and  $500\text{mm}$  to assess the effects of different wind speeds on the propeller-induced flow deflection. This was conducted at  $V=4, 6$  and  $8\text{m/s}$ , where  $\lambda=7.78, 5.19$  and  $3.89$  respectively. Each of these flow speeds was tested at  $\Phi=0, 15$  and  $30$  degrees. These configurations represented a range of operating conditions that an MUAS would experience while hovering.

For a given  $\lambda$ ,  $\alpha$  was found to reduce as  $\Phi$  was increased, which may be caused by the propeller thrust vector becoming more in-line with the wind flow vector at higher angles of attack and therefore causing less vertical deflection. This is noticeable between the results shown in Figure ?? and Figure ??. However, at each value of  $\Phi$ ,  $\alpha$  was found to become rel-

atively constant beyond  $X=400\text{mm}$ , with the difference being within experimental error. As a result, it could be determined that the effect of  $\Phi$  on beyond  $X=400\text{mm}$  could be regarded as being insignificant.

It can be seen in Figure ?? that  $\alpha$  decreases as  $\lambda$  is decreased at a given value of  $X$ . As  $V$  is increased, the longitudinal component of the flow velocity,  $u$ , is increased. Therefore, for a given propeller-induced fluctuation of the vertical velocity component,  $w$ , an increase in  $u$  will reduce the perceived  $\alpha$  angle measured by the probe. Despite the significant flow angle deflections, the flow acceleration caused by the propellers was found to be less than  $0.1\text{m/s}$ , or less than 2%, at all longitudinal positions. As a result, flow speed was not used as a deciding factor in the probe mounting position.

### 3.3.2 Calibration Offset Functions

As it was determined that operating a MHPP outside the effects of propeller wash was structurally impractical, the feasibility of actively offsetting the propeller-induced effects on the measurements taken by a MHPP was investigated. The flow field measurements in the vertical plane had demonstrated good repeatability. Surfaces were fitted to the data points to allow the function  $\alpha = f(\Phi, \lambda)$  to be calculated for arbitrary  $\Phi$  and  $\lambda$ . These surfaces were determined to be 2nd-3rd order polynomials. The surfaces could be calculated at different values of  $X$ , however ultimately only one value of  $X$  was required once the probe mounting location had been finalized. Therefore this offset method investigated using these calibration surfaces to interpolate the resultant effect of the propellers on the measured flow angle using sensor measurements, thereby allowing an angle offset to be applied in real time.

All of the required parameters could theoretically be measured onboard an MUAS using different sensors. It was found that the propellers did not have a significant impact on the measured flow speed,  $u$ . Therefore the tip speed ratio,  $\lambda$ , would be able to be determined using flow speed measured by the MHPP as well as RPM measured by onboard tachometers. The MUAS angle of attack,  $\alpha$ , could be measured using the

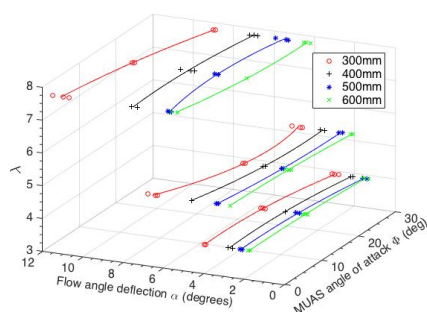


Figure 11: An example of the correction curves used to interpolate  $\alpha$  from  $\Phi$ ,  $\lambda$  and  $X$

onboard IMU. This would allow to be resolved for a MHPP mounting location, i.e.  $X$  as shown in Figure 3. The frequency at which corrections could be applied would depend on the sampling rate of each of the required sensors, and the accuracy would also be dependent on the coarseness of the calibration functions. For this project it was decided to apply the calibration offsets to mean angle measurements taken at fixed combinations of  $\Phi$ ,  $\lambda$  and  $X$ . Application and accuracy of these initial correction functions to the on-board MHPP sensor in both statically-mounted and flying configurations will be covered in the next edition of this research project. Incorporation of yaw angles and differential thrust into the correction functions will be conducted in future research in order to correct for wind measurements that are not closely aligned with the vertical plane of the MUAS. The current calibration model has been developed using time-average flow measurements at fixed attitudes with the assumption that the MUAS will hold relatively stable hover in wind. Therefore the effects of the dynamic motion of the MUAS in turbulent conditions on the accuracy of the resultant measurements will need to be investigated. These effects include the impact of the angular velocity of the probe tip on differential pressure measurements during rapid pitching due to the long probe moment arm, as well as the impact of rapidly changing the propeller tip speed differentially during changes in attitude.

#### 4 CONCLUSIONS

In order to investigate the ability of a Multi-rotor Unmanned Aerial System (MAUS) to measure atmospheric winds, the flow around a typical MUAS was studied in a series of wind tunnel tests that replicated steady-state hover and forward flight. A multi-hole pressure probe (MHPP) was used to quantify propeller-induced flow angle as a function of tip speed ratio, MUAS angle of attack and longitudinal position forwards of the MUAS. It was determined that the on-board sensor would need to be mounted more than 7 rotor radii forwards of the hub axis to avoid all induced flow effects, which was considered to be structurally impractical. However, it was determined that the induced effects were

relatively small at  $X=400\text{mm}$ , or approximately 2.5 rotor radii, and could be corrected for. This position also presented a feasible sensor mounting location without impeding MUAS maneuverability or inducing adverse deflections. Correction functions were developed from the flow field measurements to be applied to the outputs of the on-board MHPP used in subsequent research projects. These functions will be applied to wind tunnel and flight tests in future research.

#### REFERENCES

- [1] Malcolm A Heath, John D Walshe, and Simon J Watson. Estimating the potential yield of small building-mounted wind turbines. *Wind Energy*, 10(3):271–287, 2007.
- [2] Sarah E Stenabaugh, Yumi Iida, Gregory A Kopp, and Panagiota Karava. Wind loads on photovoltaic arrays mounted parallel to sloped roofs on low-rise buildings. *Journal of Wind Engineering and Industrial Aerodynamics*, 139:16–26, 2015.
- [3] RP Hoxey and PJ Richards. Flow patterns and pressure field around a full-scale building. *Journal of Wind Engineering and Industrial Aerodynamics*, 50:203–212, 1993.
- [4] C White, EW Lim, S Watkins, A Mohamed, and M Thompson. A feasibility study of micro air vehicles soaring tall buildings. *Journal of Wind Engineering and Industrial Aerodynamics*, 103:41–49, 2012.
- [5] Simon Watkins, Ee Wei Lim, and Raj Ladani. The velocity field around the top of a tall building; model-scale and full-scale measurements. *6th European and African Conference on Wind Engineering*, 2013.
- [6] Bert Blocken. 50 years of computational wind engineering: Past, present and future. *Journal of Wind Engineering and Industrial Aerodynamics*, 129:69–102, 2014.
- [7] E.W. Lim, S. Watkins, R. Clothier, R. Ladani, A. Mohamed, and J Palmer. Full-scale flow measurement on a tall building with a continuous-wave doppler lidar anemometer. *Journal of Wind Engineering and Industrial Aerodynamics*, 154:69–75, 2016.
- [8] B Canadillas, A Westerhellweg, and T Neumann. Testing the performance of a ground-based wind lidar system: One year intercomparison at the offshore platform fino1. *DEWI Magazine*, 38:58–64, 2011.
- [9] Luke Wallace, Arko Lucieer, Christopher Watson, and Darren Turner. Development of a uav-lidar system with application to forest inventory. *Remote Sensing*, 4(6):1519–1543, 2012.

- [10] Pascal Gohl, Michael Burri, Sammy Omari, Joern Rehder, Janosch Nikolic, Markus Achtelik, and R Siegwart. Towards autonomous mine inspection. In *Applied Robotics for the Power Industry (CARPI), 2014 3rd International Conference on*, pages 1–6. IEEE, 2014.
- [11] Javier Moyano Cano. *Quadrotor UAV for wind profile characterization*. PhD thesis, Universidad Carlos III de Madrid. Departamento de Informtica, 2013.
- [12] Patrick Neumann, Matthias Bartholmai, Jochen H Schiller, Burkhard Wiggerich, and Manol Manolov. Micro-drone for the characterization and self-optimizing search of hazardous gaseous substance sources: A new approach to determine wind speed and direction. In *Robotic and Sensors Environments (ROSE), 2010 IEEE International Workshop on*, pages 1–6. IEEE, 2010.
- [13] Matthew Marino, Alex Fisher, Reece Clothier, Simon Watkins, Samuel Prudden, and Chung Sing Leung. An evaluation of multi-rotor unmanned aircraft as flying wind sensors. *International Journal of Micro Air Vehicles*, 7(3):285–299, 2015.
- [14] Derrick W Yeo, Nitin Sydney, D Paley, and Donald Sofge. Onboard flow sensing for downwash detection and avoidance with a small rotor helicopter. In *Proc. AIAA Guidance Navigation and Control Conference*, 2015.
- [15] Ian de Boisblanc, Nikita Dodbele, Lee Kussmann, Rahul Mukherji, Doug Chestnut, Stephanie Phelps, Gregory C Lewin, and Stephan de Wekker. Designing a hexacopter for the collection of atmospheric flow data. In *Systems and Information Engineering Design Symposium (SIEDS), 2014*, pages 147–152. IEEE, 2014.
- [16] A Mohamed. *Phase-Advanced Attitude Sensing and Control For Fixed-Wing Micro Aerial Vehicles in Turbulence*. PhD thesis, RMIT University, 2015.
- [17] J Milbank, B Loxton, S Watkins, and WH Melbourne. *Replication of Atmospheric Conditions for the Purpose of Testing MAVs: MAV Flight Environment Project Final Report*. Royal Melbourne Institute of Technology, 2005.
- [18] Sridhar Ravi. *The influence of turbulence on a flat plate airfoil at Reynolds numbers relevant to MAVs*. PhD thesis, RMIT University Melbourne, 2011.
- [19] Turbulent Flow Instrumentation. Cobra Probe, 2016, <http://www.turbulentflow.com.au/Products/CobraProbe/CobraProbe.php>.